The Acoustical Society of Japan

J. Acoust. Soc. Jpn. (*E*) **5**, 1 (1984)

Harmonic generation mechanism in organ pipes

Shigeru Yoshikawa

5th Research Center, Technical R & D Institute, Japan Defense Agency,
3–13–1, Nagase, Yokosuka, Kanagawa, 239 Japan

(*Received 21 April 1983*)

A whole view on the harmonic generation in organ pipes is presented. It consists of elementary processes: (a) excitory source spectrum generation by the jet, (b) filtration by the inharmonic normal modes of the passive system, and (c) radiation from the pipe ends. Lateral jet velocity distribution is responsible for the source spectrum. Filtration and radiation emphasize the resultant source spectrum. Harmonic generation mechanism is classified into the unsaturated and saturated regimes, and formulated on the basis of current- and pressure-drive models. Theoretical consideration deduced: (1) Contribution of the pressure-drive to the harmonic generation is not significant. (2) Harmonic structure and its development in the unsaturated regime are defined by the matrix of the jet offset and the vector of the jet deflection amplitude. (3) A decisive factor determining the harmonic structure in the fully saturated regime is the time interval ratio of the jet switching action.

PACS number: 43. 75. Np

1. INTRODUCTION

Musical amusement becomes rich by virtue of the great variety of tone colour. Physical mechanism forming the harmonic structure, which arises a sensation of tone colour, is one of most interesting subjects in musical acoustics. The purpose of this paper is to gain a brief picture of this mechanism which is common to air-jet instruments such as organ flue pipe, recorder, flute, and Japanese shakuhachi. Fundamental aspects involved in it will be illustrated on the basis of our knowledge of the sounding mechanism in organ pipes.

Interaction between the air jet issued from the flue and the air column confined in the pipe sustains sound excitation. The viewpoints of "feedback principle" in the current-drive model[1–3] and "negative resistance" in the pressure-drive model[4] have been successfully applied to the precise description of the interaction phenomenon in the linear operation. The air jet travels across the open mouth of the pipe and then impinges on the edge. Acoustic disturbance at the mouth deflects the jet alternately inside and outside the pipe across the edge. The jet flow is thus modulated and enters the pipe to drive one of its resonance modes. The resulting resonance in turn reacts upon the jet.

Generally speaking, sounding mechanism should involve harmonic generation mechanism intrinsically. But theoretical consideration on the sounding mechanism has been restricted almost within the frequency domain (e.g., determination of sounding frequency, and phase relationship between oscillations of the jet and the column) except a few works.[5,6] The sounding mechanism needs further developing to understand many problems in the amplitude domain (e.g., formation of harmonic structure, response of attack transient, and calculation of radiated sound power from the information on the jet and pipe).

Harmonic generation in organ pipes is principally attributed to the jet-side rather than the pipe-side. Air column in the pipe is generally regarded as a linear system, and its resonance characteristics function as a kind of filter because normal mode frequencies of column resonance do not coincide

NII-Electronic Library Service

The Acoustical Society of Japan

with the harmonics of sounding frequency. On the other hand, the jet behaves like a nonlinear system[6] and must be a source of harmonics.

However, the deflecting oscillation of the jet over the mouth is assumed to be almost linear. Good agreement on the wafted shape of the jet is obtained between the theories[1,3] in which only fundamental component with sounding frequency is considered and the experiments[3,4] which show the snapshots of the wafted jet in real situation. According to the theory,[1] the oscillatory displacement of the wafted jet is inversely proportional to the square of sounding frequency. The waft of the jet due to harmonic components may thus be strongly weakened. Moreover, according to the theory on the jet instability,[7] the condition which assures an oscillatory jet flow with growing amplitude becomes much severer for harmonic components. From these reasons we do not lose the adequacy of treatment even when harmonic components of the jet oscillation are neglected. We must therefore consider that the harmonic generation does not originate in the nonlinearity of jet oscillation but in other aspects of the jet.

By the way, an experimental work[8] investigated the relationship between the harmonic level and the offset of the jet center plane relative to the edge. From its result we can state that the cause of harmonic generation is the deflecting action of the offset jet across the edge. Moreover, it is well known that organ builders adjust the "voicing" by properly changing the jet offset from their own experiences.[9] From such a point of view, Fletcher and Douglas[10] mathematically formulated the harmonic generation by the above action. Independently of them, the present author[11] also proposed a similar formulation with different mathematical expression.

In this paper, the previous formulation[11] on the source spectrum originated in the deflecting action of the jet is further developed. Our treatment involves the current- and pressure-drive models. Sounding regime is classified into the unsaturated and saturated regimes. Moreover, the filtering function of air column resonance and radiation characteristic of open ends, which transform the source spectrum, are included. In order to understand the filtered and radiated spectrums, an ideal model of uniform tube is adopted.

Our simplified theory along the above general approach will bring the overall view of harmonic generation in organ pipes, although its experimental confirmation is postponed in the future. Real situation of harmonic generation will be inferred from the actualization and complication of the above elementary processes: source spectrum generation, filtration, and radiation.

2. SOURCE SPECTRUM OF THE JET

2.1 Source Spectrum Due to the Current-Drive

Traveling across the open mouth, the jet flow gradually slows down and laterally spreads out because of mixing between the jet and the surrounding still air. In the previous paper,[1] the authors included the slowdown of the jet in the theory, while excluded the lateral spread intentionally. Such a simplified model was most effective to describe the phase relation between the oscillations of air jet and air column, and to construct a fundamental theory on the organ pipe sounding mechanism.

Starting-point of this paper is then the established steady state oscillation of the spread jet across the edge (Fig. 1). The offset of the symmetry plane of the jet relative to the edge is expressed as y_0. Asymmetrical jet-edge configuration due to this offset is general in real organ pipes.

At the edge, we suppose the following lateral velocity distribution of the jet:

$$U(y)=U_e g(y/\sigma)=U_e g(\eta), \quad \eta=y/\sigma. \qquad (1)$$

The distribution $g(\eta)$ is assumed to be symmetrical for the simplicity. The quantity σ is a constant for normalization, which means a quantity like the

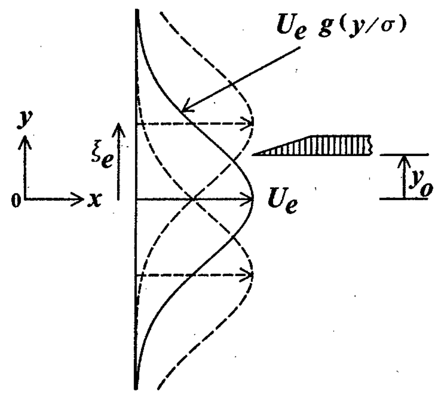

Fig. 1 Asymmetrical jet-edge configuration with the offset y_0.
The jet has lateral velocity distribution $U_e g(y/\sigma)$ at the edge (located at $x=d$, $y=y_0$), and swings up and down across it with the alternating displacement $\xi_e(t)$.

NII-Electronic Library Service

The Acoustical Society of Japan

standard deviation of distribution and indicates the effective thickness of the jet. The value U_e is the velocity at the jet center plane ($y=0$). The origin of our coordinate is set at the center of the flue slit from which the jet emerges. The position of the edge is then given by $x=d$ and $y=y_0$. The value d is called the lip cut-up or slit-to-edge distance, and y_0 the offset of the jet.

Because the jet swings up and down across the edge with the alternating displacement $\xi_e(t)$, we can define the driving current Q_e to the pipe as the following acoustic volume flow:

$$Q_e(t)=(bU_e)\int_0^{y_0-\xi_e(t)} g(y/\sigma)dy$$
$$=(b\sigma U_e)\int_0^{\eta_0-\eta_e(t)} g(\eta)d\eta\,, \qquad (2)$$

where b is the jet width, η_e the normalized jet oscillation $\xi_e(t)/\sigma$, and η_0 the normalized offset y_0/σ. Note that the positive direction of $\xi_e(t)$ is drawn from the inside to the outside of the pipe, and that a half of total flow is neglected since it has no acoustical importance.

The jet oscillation itself may hardly contains harmonic components as mentioned in Introduction. It is thus safe to consider that the jet oscillation $\xi_e(t)$ at the edge takes the linear form:

$$\xi_e(t)=\hat{\xi}_e\cos(\omega_s t+\delta) \qquad (3)$$

with the amplitude $\hat{\xi}_e$, the sounding frequency $\omega_s/2\pi$, and the initial phase δ. Taking a normalized expression, we get

$$\eta_e(t)=\hat{\eta}_e\cos(\omega_s t+\delta)\,. \qquad (4)$$

If the jet driving current $Q_e(t)$ given by Eqs. (2) and (4) shows a periodic oscillation, we may expand it in Fourier series:

$$Q_e(t)=(b\sigma U_e)\sum_{n=0}^{\infty}\hat{q}_n\cos[n(\omega_s t+\delta)]\,, \qquad (5)$$
$$\hat{Q}_{en}=(b\sigma U_e)\hat{q}_n\,. \qquad (6)$$

Absolute amplitude of $\hat{Q}_{en}$ (for $n=1, 2, 3, \cdots$) defines the level of source spectrum due to the current-drive, and absolute value of $\hat{q}_n$ the relative level of that. Note that $\hat{q}_n$ in Eq. (5) can take the negative value. The unusual expression of Eq. (5) with such an additional condition is adopted for the algebraic advantage [cf. Eq. (33) in Sec. 5].

Performance of the integral in Eq. (2) depends upon the functional form of distribution $g(\eta)$. Since our purpose is the understanding of funda-

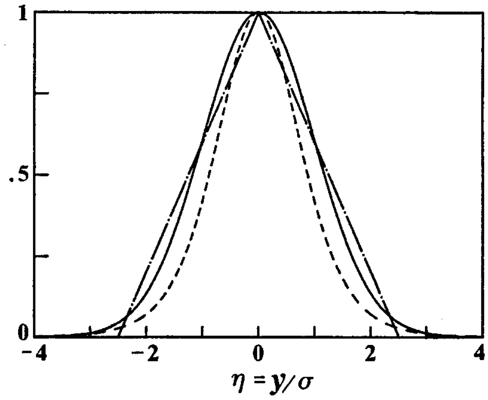

Fig. 2 Approximate distributions of the jet velocity.
——, $\exp(-\eta^2/2)$; – – –, $\mathrm{sech}^2(\eta)$; and —·—, $1-(|\eta|/\sqrt{2\pi})$.

mental aspects in the harmonic generation, physical rigidity on the form of $g(\eta)$ is not necessary, then we may favorably adopt any rational form (cf. Fig. 2) to make the integral calculation easy. Fully developed jet flow has the Gaussian distribution, which is adopted to perform the integral in this paper. Laminar jet usually has the form $\mathrm{sech}^2(\eta)$, which has the algebraic advantage because the integral of sech^2 is tanh.[10] Triangular form gives a relatively close approximation to the above two.[12] In real organ pipes, the jet probably behaves like a turbulent flow because of its high speed and the "nicking" on the languid. While such a turbulent flow does not have the above profiles exactly, they give sufficient approximations to serve our purpose.

2.2 Source Spectrum Due to the Pressure-Drive

Another type of source spectrum is derived from the pressure-drive model[4] of sounding mechanism, although the former one due to the current-drive model is dominant in most cases.[1,2] Conservation of momentum flow flux on the deflecting jet deduces the sound pressure $p_e(t)$ which drives the pipe:

$$p_e(t)=\rho U_e^2[-b\xi_e(t)/S_p]\,, \qquad (7)$$

where ρ is the air density and S_p the cross sectional area of the pipe.

Taking the jet velocity profile $g(\eta)$ into consideration, we can obtain the generalized expression

$$p_e(t)=(b\sigma/S_p)(\rho U_e^2)\int_0^{\eta_0-\eta_e(t)}[g(\eta)]^2d\eta\,. \qquad (8)$$

Fourier series expansion of Eq. (8) gives the level of source spectrum $|\hat{p}_{en}|$ (for $n=1, 2, 3, \cdots$) due to the pressure-drive:

NII-Electronic Library Service

The Acoustical Society of Japan

$$p_e(t)=(b\sigma/S_p)(\rho U_e^2)\sum_{n=0}^{\infty}\hat{p}_n\cos[n(\omega_s t+\delta)]\,, \quad (9)$$

$$\hat{p}_{en}=(b\sigma/S_p)(\rho U_e^2)\hat{p}_n\,. \quad (10)$$

In the latter section, we illustrate numerical example of both source spectrums $\hat{Q}_{en}$ and $\hat{p}_{en}$ (or $\hat{q}_n$ and $\hat{p}_n$) by adopting the Gaussian profile for the jet velocity distribution.

3. FILTERED SPECTRUM

Acoustic excitory sources Q_e and p_e produce the acoustic flow Q_p into the pipe. Using source spectrums $\hat{Q}_{en}$ and $\hat{p}_{en}$ given by Eqs. (6) and (10) respectively, we obtain the spectrum $\hat{Q}_{pn}$ of this pipe flow as follows[2,18]:

$$(\hat{Q}_{pn})=(\hat{Q}_{pn})_{\rm I}+(\hat{Q}_{pn})_{\rm II}\,, \quad (11)$$

$$(\hat{Q}_{pn})_{\rm I}=[Z_{mn}/(Z_{pn}+Z_{mn})]\hat{Q}_{en}\,, \quad (12)$$

$$(\hat{Q}_{pn})_{\rm II}=[1/(Z_{pn}+Z_{mn})]\hat{p}_{en}\,, \quad (13)$$

where Z_{pn} is the value of the acoustic impedance of the pipe with both open end corrections evaluated at the nth harmonic, and Z_{mn} that of both the mouth and the jet wafting over the mouth evaluated at the nth harmonic; i.e., $Z_{pn}=Z_p(n\omega_s)$ and $Z_{mn}=Z_m(n\omega_s)$. In this sense, we call Z_{pn} and Z_{mn} the nth Fourier components of acoustic impedances Z_p and Z_m respectively. Although acoustic impedance of the jet plays an essential role in the sounding mechanism,[1] we here neglect it for the simplicity because its magnitude is relatively smaller than that of mouth impedance in most conditions. Moreover, note that minor spectrum due to quadratic terms[2,18] of jet deflection ξ_e is excluded from Eq. (11).

Fourier components of pipe and mouth impedances are respectively expressed as[2]

$$Z_{pn}=(\rho c/S_p)[H_n+j\tan(k_nL)]/[1+jH_n\tan(k_nL)]\,, \quad (14)$$

$$Z_{mn}\simeq j(\rho c/S_p)(k_n\Delta l)\,, \quad (15)$$

where $k_n=nk_1=n(\omega_s/c)$ and $H_n=\tanh(k_nL/2Q_N)$. The quantities L and Δl are effective lengths of pipe and mouth respectively, whose frequency dependence is neglected. The quantity k_n is the nth harmonic wave number, c the sound velocity in the pipe, and Q_N the Q-value of Nth normal mode resonance of the pipe. Discriminate the subscript N from n. The subscript n indicates a harmonic series or Fourier component, while the N a normal mode series.

Using Eqs. (6), (10), (14), and (15), we rewrite Eqs. (12) and (13) respectively:

$$(\hat{Q}_{pn})_{\rm I}=[(b\sigma U_e)\hat{q}_n][(j\omega_s\Delta l/c)nY_n]\,, \quad (16)$$

$$(\hat{Q}_{pn})_{\rm II}=[(b\sigma U_e)\hat{p}_n][(U_e/c)Y_n]\,, \quad (17)$$

where

$$Y_n=[1/(Z_{pn}+Z_{mn})](\rho c/S_p)\,. \quad (18)$$

The function Y_n corresponds to the total admittance $1/(Z_{pn}+Z_{mn})$ normalized by the characteristic acoustic impedance $\rho c/S_p$ of the pipe. Note that $(\hat{Q}_{pn})_{\rm I}$ is proportional to nY_n, while $(\hat{Q}_{pn})_{\rm II}$ to only Y_n. From Eqs. (16) and (17) we know that the ratio $|(\hat{Q}_{pn})_{\rm I}/(\hat{Q}_{pn})_{\rm II}|$ may be given by $n\omega_s\Delta l/U_e$ because $\hat{q}_n$ and $\hat{p}_n$ have almost the same order of magnitude as illustrated in latter section. The current-drive is therefore predominant for both high sounding frequencies and higher order of harmonics, while the pressure-drive becomes predominant for high jet velocities or high blowing pressures.

Figure 3 shows an example of the magnitude of normalized total admittance by using the continuous variable $k(=\omega/c)$ instead of the discrete one $k_n(=n\omega_s/c)$ in Eqs. (14) and (15). Following numerical values have been assumed to draw Fig. 3: sounding frequency $f_s=\omega_s/2\pi=200$ Hz, pipe diameter $D=3$ cm, and effective mouth length $\Delta l=L/20$. The

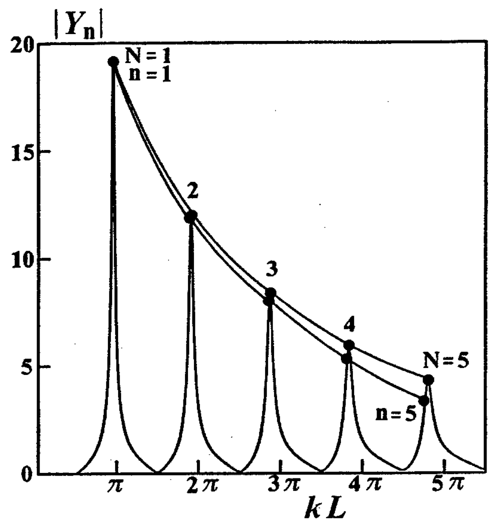

Fig. 3 Magnitude of normalized total admittance $|Y_n|$ of the pipe-mouth system. A harmonic series $(n=1, 2, \cdots)$ departs from a normal mode series $(N=1, 2, \cdots)$ given by admittance peaks. Numerical data: sounding frequency $f_s=200$ Hz, pipe diameter $D=3$ cm, and ratio of effective mouth length to effective pipe length $\Delta l/L=1/20$.

NII-Electronic Library Service

The Acoustical Society of Japan

Q-value of each mode resonance is calculated from Eqs. (19) and (20) shown below. The discordancy between a harmonic series and a normal mode series is clearly illustrated in Fig. 3 where the sounding frequency or the first harmonic ($n=1$) is assumed to coincide with the fundamental resonance frequency or the first normal mode frequency ($N=1$) which is given by $kL=0.953\pi$. The harmonic series therefore consists of $kL=0.953\pi$, 1.906π, 2.859π, 3.812π, 4.765π, $\cdots$, while the normal mode series consists of $kL=0.953\pi$, 1.908π, 2.866π, 3.830π, 4.799π, $\cdots$ as the numerical calculation on the peaks of $|Y_n|$ shows.

For the above calculation we have employed the following relation on the Q-value:

$$Q_N \simeq [\alpha/(\sqrt{Nf_s}\,D)+\beta(Nf_s{}^2D^2)]^{-1}, \tag{19}$$

where α and β are numerical coefficients. Equation (19) shows the fact that the dissipation of acoustic energy in a pipe is principally due to two causes.[14,15] The first is the so-called wall boundary effect which brings viscous and thermal losses to the pipe wall, and expressed as the first term in the right-hand side of Eq. (19). The second is the sound radiation from the mouth and open end, and expressed as the second term in the right-hand side of Eq. (19).

Theoretical expressions of α and β are of course possible, while the experimental determination of their values is more effective in most cases. According to Benade,[14] we have

$$\alpha \simeq 1.4\,, \quad \beta \simeq 3\times 10^{-9}\,, \tag{20}$$

if pipe diameter D is given in centimeters. Using the assumed values $D=3$ and $f_s=200$, we get $Q_1=29$, $Q_2=39$, $Q_3=45$, $Q_4=48$, and $Q_5=50$ from Eqs. (19) and (20). Wall losses are usually dominant, but radiation losses become large as the sounding frequency, mode number, and pipe diameter increase respectively. The mode number at which radiation losses surpass wall losses is given by

$$N \simeq 6\times 10^5 f_s{}^{-5/3} D^{-2} \tag{21}$$

from Eqs. (19) and (20). In the case of Fig. 3 this $N=10$.

A normal mode series, which is defined by the peaks of $|Y_n|$, shows the anharmonicity as illustrated in Fig. 3. Such mode dependence of Q-value as expressed by Eq. (19) causes this anharmonicity. The degree of anharmonicity of Nth mode resonance may increase with the increasing N. Therefore higher harmonics tend to strongly depend on the Q-value of the corresponding normal mode. Mouth length Δl also affects the harmonic content. Large Δl may reduce higher harmonics by lowering the sounding frequency.

Generally speaking, harmonic source spectrum of the jet is more or less affected by the inharmonic normal mode of the passive system which consists of the pipe and mouth. Such an effect becomes quite uneven when the system undergoes any geometrical modification e.g., partly widening and narrowing of the pipe.[16] We may thus consider that the individual normal mode operates as a kind of filter. Then we will define the spectrum of pipe flow $\hat{Q}_{pn}$ given by Eq. (11) as the filtered spectrum. And the filtration is characterized by the normalized total admittance Y_n.

4. RADIATED SOUND SPECTRUM

Sound radiation takes place at the mouth and pipe-end openings. Acoustic flow through the mouth opening is given by $-\hat{Q}_{pn}$ when $\hat{Q}_{pn}$ gives the acoustic flow into the pipe.[1] Acoustic flow through the end opening is approximately given by $-\hat{Q}_{pn}$ and $\hat{Q}_{pn}$ for odd and even modes respectively. That is, odd harmonics radiate in phase from above two openings, while even harmonics out of phase.

In the free field, sound radiation from organ pipes is thus regarded as that from two point sources insofar as the opening is relatively small compared to the wavelength (cf. Fig. 4). Therefore we receive the following sound pressure at point (r, θ):

$$p_n(r,\theta)=j[\rho(n\omega_s)/4\pi](-\hat{Q}_{pn}) \cdot\left(\frac{e^{-jk_n r_E}}{r_E}\pm\frac{e^{-jk_n r_M}}{r_M}\right), \tag{22}$$

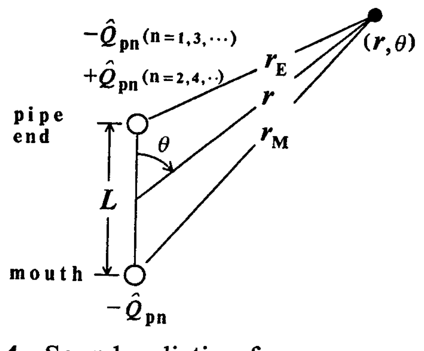

Fig. 4 Sound radiation from an organ flue pipe.
Pipe end and mouth approximately operate as a monopole respectively.

NII-Electronic Library Service

The Acoustical Society of Japan

where the plus sign is used for odd harmonics and the minus sign for even harmonics. In the far field ($r \gg L$), Eq. (22) is rewritten as

$$p_n(r,\theta)=j[\rho(n\omega_s)/4\pi](-2\hat{Q}_{pn}) \cdot \begin{Bmatrix}\cos\\ j\sin\end{Bmatrix}[(k_nL/2)\cos\theta]\frac{e^{-jk_nr}}{r}, \qquad (23)$$

where the cos is used for odd harmonics and the $j$sin for even harmonics.

Let us define the level of radiated sound spectrum $|\hat{p}_{rn}|$ by setting $r=1$ and $\left|\begin{matrix}\cos\\ \sin\end{matrix}[(k_nL/2)\cos\theta]\right|=1$ in Eq. (23):

$$|\hat{p}_{rn}|=[\rho(n\omega_s)/4\pi]|2\hat{Q}_{pn}|. \qquad (24)$$

This equation tells us that the filtered spectrum $\hat{Q}_{pn}$ suffers an emphasis of higher harmonics, proportional to n, through the radiation.

We can write down the radiated sound spectrum as follows by using Eqs. (11), (16), and (17):

$$\hat{p}_{rn}=(\hat{p}_{rn})_{\mathrm{I}}+(\hat{p}_{rn})_{\mathrm{II}}, \qquad (25)$$

$$(\hat{p}_{rn})_{\mathrm{I}}=[(b\sigma U_e)\hat{q}_n][j(2\pi f_s\Delta l/c)nY_n][(\rho f_s)n], \qquad (26)$$

$$(\hat{p}_{rn})_{\mathrm{II}}=[(b\sigma U_e)\hat{p}_n][(U_e/c)Y_n][(\rho f_s)n], \qquad (27)$$

where $(\hat{p}_{rn})_{\mathrm{I}}$ and $(\hat{p}_{rn})_{\mathrm{II}}$ are the radiated sound spectrums due to the current- and pressure-drives respectively. Note that the former has a phase advance of $\pi/2$ relative to the latter if the $\hat{q}_n$ and $\hat{p}_n$ (for $n=1, 2, 3, \cdots$) have the same sign each other. This is attributed to the phase difference between the maximums of acoustic current and pressure in a pipe. According to Eqs. (26) and (27), an excitory source spectrum $\hat{Q}_{en}$ (or $\hat{q}_n$) suffers an emphasis of higher harmonics which is proportional to n^2Y_n, while another one $\hat{p}_{en}$ (or $\hat{p}_n$) suffers an weaker emphasis proportional to nY_n. Using the same parameter values as in Fig. 3, we draw the curve of emphasis $n^2|Y_n|$ in Fig. 5.

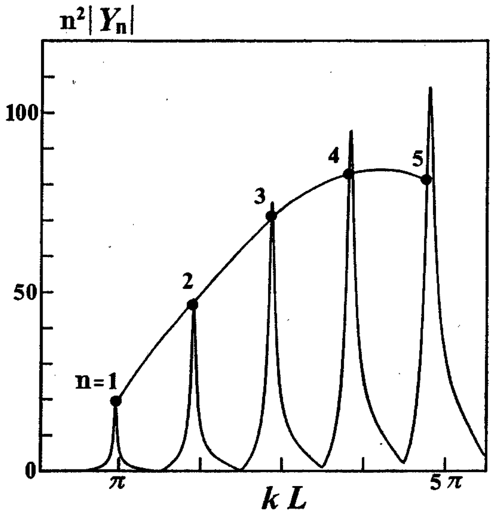

Fig. 5 Emphasis curve $n^2|Y_n|$ of radiated sound spectrum due to the current-drive. Numerical data are the same as in Fig. 3.

Summing up, above Eqs. (26) and (27) formulate the elementary processes in the harmonic generation: excitory source spectrum generation by the jet, filtration by the normal modes of the passive pipe-mouth system, and radiation from the open ends.

5. UNSATURATED REGIME

Harmonic generation in organ flue pipes essentially depends on the alternating deflection of the jet. Even if the amplitude of this deflection continues to grow, the saturation of the jet flow into the pipe necessarily occurs. When the jet is deflected in a sinusoidal way with a small amplitude, the jet flow does not yet saturate. As the amplitude becomes large, the jet begins to blow completely outside or inside the pipe, and the saturation comes about. First we treat the deflecting jet with such an amplitude that does not bring the saturation in this section, and second the completely switching jet with a sufficiently large amplitude to saturate the jet flow in the next section.

5.1 Calculation of Jet Source Spectrum

Taylor expansion around null deflection ($\eta_e=0$) rather than Fourier series expansion may be more effective method to calculate integrals (2) and (8):

$$Q_e=(b\sigma U_e)\left\{\int_0^{\eta_0}g(\eta)d\eta + \sum_{n=1}^{\infty}[g^{(n-1)}(\eta_0)/n!][\eta_e(t)]^n\right\}, \qquad (28)$$

$$p_e=(b\sigma/S_p)(\rho U_e^2)\left\{\int_0^{\eta_0}g^2(\eta)d\eta + \sum_{n=1}^{\infty}[g^{2,(n-1)}(\eta_0)/n!][\eta_e(t)]^n\right\}, \qquad (29)$$

where

$$g^{(n)}(\eta_0)=[d^ng(\eta_0-\eta_e)/d\eta_e{}^n]_{\eta_e=0} =(-1)^n[d^ng(\eta)/d\eta^n]_{\eta=\eta_0}, \qquad (30)$$

$$g^{2,(n)}(\eta_0)=(-1)^n[d^ng^2(\eta)/d\eta^n]_{\eta=\eta_0}. \qquad (31)$$

Above equations tells us that the higher derivatives of the velocity distribution function evaluated at

NII-Electronic Library Service

The Acoustical Society of Japan

the edge position ($\eta=\eta_0$) yield the source spectrum of the jet.

As a simple example we take the following Gaussian distribution of the jet velocity (cf. Fig. 2):

$$g(\eta)=\exp(-\eta^2/2)\,. \tag{32}$$

From Eqs. (30) and (31) we get

$$g^{(n)}(\eta_0)=e^{-\eta_0^2/2}\sum_{r=0}^{[n/2]}\frac{(-1)^{2n-r}n!}{2^r(n-2r)!\,r!}(\eta_0)^{n-2r}\,,$$

$$g^{2,(n)}(\eta_0)=e^{-\eta_0^2}\sum_{r=0}^{[n/2]}\frac{(-1)^{2n-r}n!}{(n-2r)!\,r!}(\eta_0)^{n-2r}\,,$$

where $[n/2]$ expresses the maximum integer not exceeding $n/2$. Then Eqs. (28) and (29) give each source spectrum for the current- and pressure-drives respectively:

$$Q_e=(b\sigma U_e)\Big\{\mathrm{erf}(\eta_0)+e^{-\eta_0^2/2}\sum_{m=0}^{[n/2]}\left[\sum_{n=0}^{\infty}\sum_{r=0}^{[n/2]}\frac{(-1)^r(\eta_0)^{n-2r}(\hat{\eta}_e)^{n+1}}{(n+1)2^{n+r}(n-2r)!\,r!}\right]\times{}_{n+1}C_m(\cos[(n+1-2m)(\omega_s t+\delta)]+\varDelta)\Big\}\,, \tag{33}$$

$$p_e=(b\sigma/S_p)(\rho U_e^2)\Big\{\frac{\sqrt{\pi}}{2}\mathrm{erf}(\eta_0)+e^{-\eta_0^2}\sum_{m=0}^{[n/2]}\left[\sum_{n=0}^{\infty}\sum_{r=0}^{[n/2]}\frac{(-1)^r(\eta_0)^{n-2r}(\hat{\eta}_e)^{n+1}}{(n+1)2^{n}(n-2r)!\,r!}\right]\times{}_{n+1}C_m(\cos[(n+1-2m)(\omega_s t+\delta)]+\varDelta)\Big\}\,, \tag{34}$$

where $\varDelta$ equals to 1/2 if n equals odd number or 0 if n equals even number, and the erf is the error function defined by $\mathrm{erf}(z)=\int_0^z\exp(-x^2/2)dx$.

Comparing Eqs. (33) and (34) with Eqs. (5) and (9) respectively, we get the explicit expression for the relative levels $\hat{q}_n$ and $\hat{p}_n$ ($n=1, 2, 3, \cdots$) of jet source spectrums. It may be effective to arrange these results in the following matrix form:

$$\begin{pmatrix}\hat{q}_1/\hat{\eta}_e^{\,1}\\ \hat{q}_2/\hat{\eta}_e^{\,2}\\ \hat{q}_3/\hat{\eta}_e^{\,3}\\ \hat{q}_4/\hat{\eta}_e^{\,4}\\ \hat{q}_5/\hat{\eta}_e^{\,5}\\ \vdots\\ \vdots\end{pmatrix}=(\eta_0)_{\mathrm{even}}g(\eta_0)\begin{pmatrix}1 & A_{12} & A_{13} & A_{14} & \cdots\\ 1 & A_{22} & A_{23} & A_{24} & \cdots\\ A_{12}/3 & A_{13}/2 & 3A_{14}/5 & \cdots & \cdots\\ A_{22}/4 & 2A_{23}/5 & A_{24}/2 & \cdots & \cdots\\ A_{13}/10 & A_{14}/5 & \cdots & \cdots & \cdots\\ \cdots & \cdots & \cdots & \cdots & \cdots\\ \cdots & \cdots & \cdots & \cdots & \cdots\end{pmatrix}\begin{pmatrix}1\\ \hat{\eta}_e^{\,2}\\ \hat{\eta}_e^{\,4}\\ \hat{\eta}_e^{\,6}\\ \vdots\\ \vdots\\ \vdots\end{pmatrix}, \tag{35}$$

$$\begin{pmatrix}\hat{p}_1/\hat{\eta}_e^{\,1}\\ \hat{p}_2/\hat{\eta}_e^{\,2}\\ \hat{p}_3/\hat{\eta}_e^{\,3}\\ \hat{p}_4/\hat{\eta}_e^{\,4}\\ \hat{p}_5/\hat{\eta}_e^{\,5}\\ \vdots\\ \vdots\end{pmatrix}=(\eta_0)_{\mathrm{even}}g^2(\eta_0)\begin{pmatrix}1 & B_{12} & B_{13} & B_{14} & \cdots\\ 1 & B_{22} & B_{23} & B_{24} & \cdots\\ B_{12}/3 & B_{13}/2 & 3B_{14}/5 & \cdots & \cdots\\ B_{22}/4 & 2B_{23}/5 & B_{24}/2 & \cdots & \cdots\\ B_{13}/10 & B_{14}/5 & \cdots & \cdots & \cdots\\ \cdots & \cdots & \cdots & \cdots & \cdots\\ \cdots & \cdots & \cdots & \cdots & \cdots\end{pmatrix}\begin{pmatrix}1\\ \hat{\eta}_e^{\,2}\\ \hat{\eta}_e^{\,4}\\ \hat{\eta}_e^{\,6}\\ \vdots\\ \vdots\\ \vdots\end{pmatrix}, \tag{36}$$

where $(\eta_0)_{\mathrm{even}}$ equals η_0 if the harmonic order n is an even number or equals 1 if n is an odd number. Matrix elements $A_{12}=(\eta_0^2-1)/8$, $A_{13}=(\eta_0^4-6\eta_0^2+3)/192$, $A_{14}=(\eta_0^6-15\eta_0^4+45\eta_0^2-15)/9216$, $A_{22}=(\eta_0^2-3)/48$, $A_{23}=(\eta_0^4-10\eta_0^2+15)/1536$, $A_{24}=(\eta_0^6-21\eta_0^4+105\eta_0^2-105)/92160$; $B_{12}=(\eta_0^2-2)/8$, $B_{13}=(\eta_0^4-12\eta_0^2+12)/192$, $B_{14}=(\eta_0^6-30\eta_0^4+180\eta_0^2-120)/9216$, $B_{22}=(\eta_0^2-6)/48$, $B_{23}=(\eta_0^4-20\eta_0^2+60)/1536$, and $B_{24}=(\eta_0^6-42\eta_0^4+420\eta_0^2-840)/92160$.

5.2 Effects of Jet Offset and Deflection Amplitude

Figure 6 shows the jet source spectrum $\hat{q}_n$ (for $n=1, 2, 3,$ and 4) of Eq. (35) as a function of the offset η_0. The amplitude of the jet deflection $\hat{\eta}_e$ as a parameter takes values 0.5, 1.0, and 1.5 respectively [from Fig. 6 it seems that Taylor expansion of Eq. (35) converges even at $\hat{\eta}_e=1.5$]. Odd harmonics $\hat{q}_1$ and $\hat{q}_3$ are both symmetrical about the axis of ordinates and have opposite signs each

NII-Electronic Library Service

The Acoustical Society of Japan

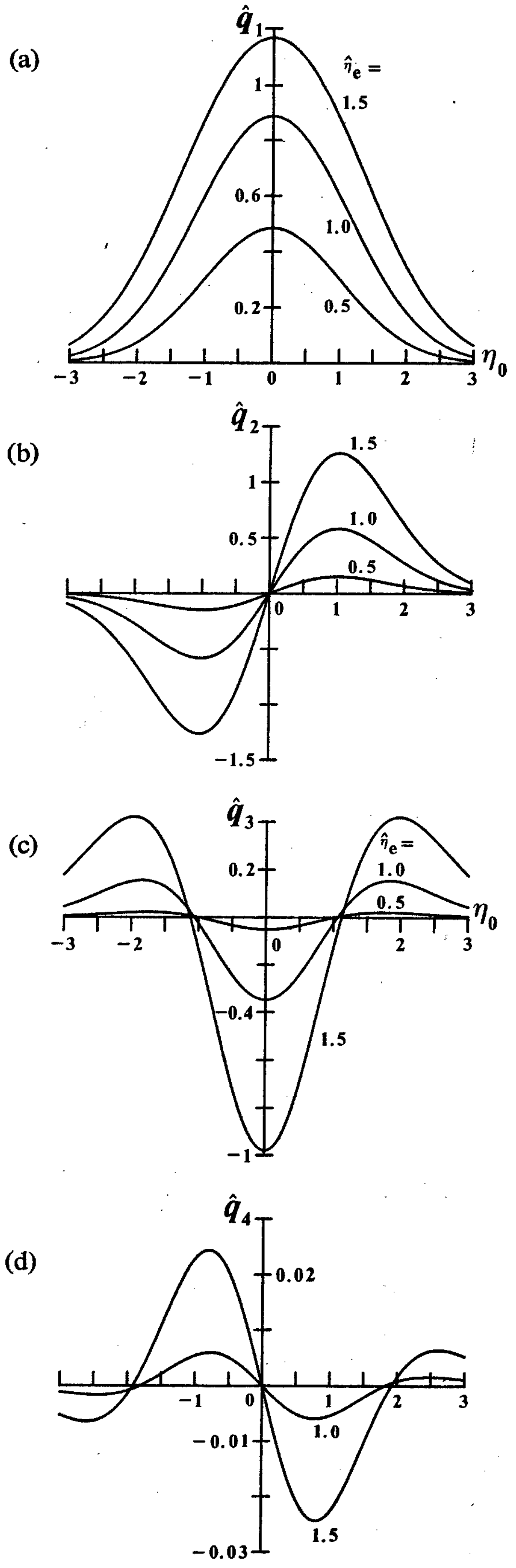

Fig. 6 Jet source spectrum $\hat{q}_n$ as a function of normalized jet offset η_0 (current-drive). Parameter is the normalized jet deflection amplitude $\hat{\eta}_e$. (a) Fundamental, (b) 2nd harmonic, (c) 3rd harmonic, and (d) 4th harmonic.

other at small offsets ($|\eta_0|<1$). On the other hand, even harmonics $\hat{q}_2$ and $\hat{q}_4$ are both symmetrical about the origin and have opposite signs each other in a relatively wide range of the offset ($|\eta_0|<1.7$). All harmonic components except fundamental one have their own zeroes. These characteristics are attributed to the nature of matrix A_{ij} ($i, j=1, 2, 3, \cdots$) which is a function of η_0 only. Calculation on $\hat{p}_n$ of Eq. (36) shows the similar result.

Following relations are approximately derived from Eqs. (6), (10), (35), and (36):

$$\hat{Q}_{en} \gg \hat{Q}_{e(n+1)},\quad \hat{Q}_{e(2n'-1)} \propto (\hat{\xi}_e)^{2n'-1},\quad \hat{Q}_{e(2n')} \propto y_0(\hat{\xi}_e)^{2n'},$$
$$\hat{p}_{en} \gg \hat{p}_{e(n+1)},\quad \hat{p}_{e(2n'-1)} \propto (\hat{\xi}_e)^{2n'-1},\quad \hat{p}_{e(2n')} \propto y_0(\hat{\xi}_e)^{2n'}$$
$$(n=1, 2, 3, \cdots;\ n'=1, 2, 3, \cdots).$$

Above relations on jet source spectrum components are held quite good for very small amplitudes of jet deflection $\hat{\xi}_e$.

But rigorously, Eqs. (35) and (36) show that the magnitudes of $\hat{q}_n$ and $\hat{p}_n$ increase with more than nth power of the normalized jet deflection $\hat{\eta}_e$. This is caused by the vector $(1, \hat{\eta}_e^2, \hat{\eta}_e^4, \hat{\eta}_e^6, \cdots)$ in the right-hand side of Eqs. (35) and (36) respectively. Hence, the amplitude of each spectrum component grows rapidly with the increasing jet deflection amplitude. This suggests an important role of the above vector in the harmonic development.

Interrelation between harmonics can be clearly understood from Figs. 7(a) and (b) where source spectrum levels $|\hat{q}_n|$ and $|\hat{p}_n|$ (for $n=1\sim5$; $\hat{\eta}_e=1.0$) are drawn respectively:

1) Odd and even harmonics respectively have their own maximums at almost same offset values.
2) Numbers of maximums and minimums (or nulls) increase with the ascending harmonic order.
3) Maximums of odd harmonics lie near minimums of even harmonics.
4) Conversely, minimums of odd harmonics lie near maximums of even harmonics.
5) Especially, zero offset gives no even harmonics but gives the highest level of each odd harmonic.
6) Intervals between neighbouring maximums (or minimums) are narrower in $|\hat{q}_n|$ than in $|\hat{p}_n|$.

The structure of matrices shown in Eqs. (35) and (36) brings above characteristics in the harmonic structure.

Matrix structure reveals that odd harmonics have their own origins (i.e., $A_{12}, A_{13}, A_{14}, \cdots; B_{12}, B_{13}, B_{14}, \cdots$) which are different from those of even harmonics

NII-Electronic Library Service

The Acoustical Society of Japan

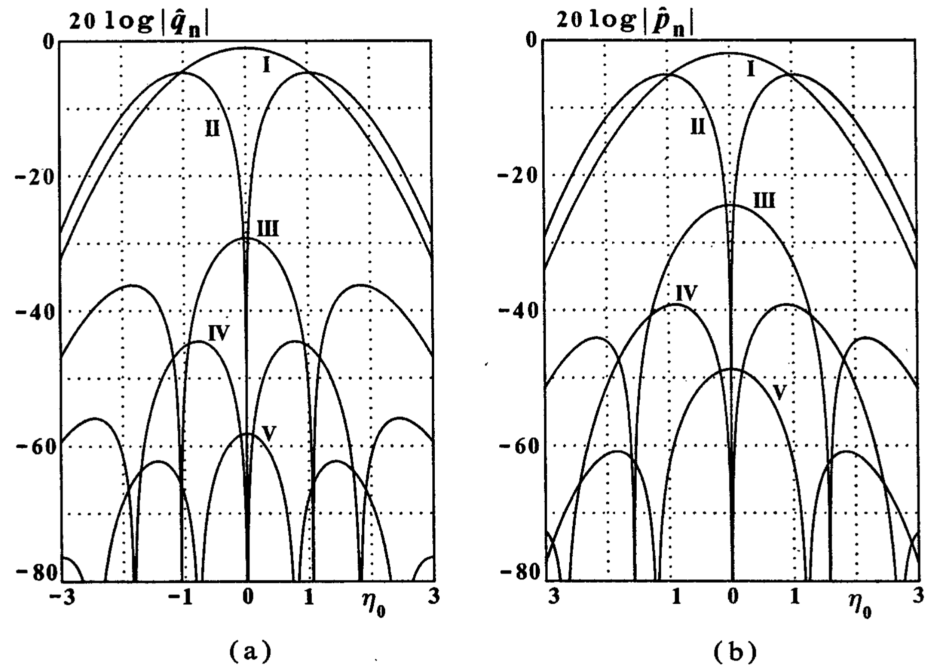

Fig. 7 Jet source spectrum level as a function of the normalized jet offset (unsaturated regime).
(a) Current-drive, (b) pressure-drive. The normalized jet deflection amplitude is assumed to be 1.0. The Roman numerals represent the harmonics (I, fundamental; II, 2nd harmonic, etc.).

(i.e., $A_{22}, A_{23}, A_{24}, \cdots; B_{22}, B_{23}, B_{24}, \cdots$). This theoretical result gives physical foundation which permits musical consideration of harmonic structure by separating it into odd and even ones.[8] Organ flue pipes will be endowed with particular tone colour according to a definite value of jet offset, since matrix elements depend only on the offset. We can thus recognize the musical importance of the offset adjustment, which principally controls the "voicing" of organ pipes.

5.3 Radiated Spectrum

After the filtration by the normal mode resonance in the pipe, jet source spectrums are radiated from the mouth and open end. According to Eqs. (26) and (27), we can illustrate the radiated spectrum levels $|(\hat{p}_{rn})_{\mathrm{I}}|$ and $|(\hat{p}_{rn})_{\mathrm{II}}|$ respectively. In Figs. 8 (a) and (b), we plot logarithmic levels $20 \log |(\hat{p}_{rn})_{\mathrm{I}}|$ and $20 \log |(\hat{p}_{rn})_{\mathrm{II}}|$ relative to 1 μPa. The value of "dB *re* 0.0002 dyn/cm^2" is given by subtracting 26 from the value of "dB *re* 1 μPa."

Geometrical and acoustical parameter values for drawing Fig. 8 are taken from an experimental model CP-I of the organ pipe in the previous paper,[1] and listed in Table 1. We have supposed that the value of effective jet thickness σ at the edge becomes three times the initial thickness at the flue slit. Q_N-values are calculated from Eqs. (19) and (20).

Table 1 Parameter values to calculate the radiated spectrum (unsaturated regime).

Normalized jet deflection	$\hat{\eta}_e$	1.0
Effective jet thickness	σ	0.6 cm
Jet width	b	1.5 cm
Jet velocity	U_e	2.5 m/s
Air density	ρ	1.2 kg/m^3
Sound velocity	c	340 m/s
Effective pipe length	L	64 cm
Effective mouth length	Δl	4 cm
Pipe diameter	D	3 cm
First normal mode	$k_1 L$	0.942 π
Sounding frequency	f_s	250 Hz
$Q_1=32$, $Q_2=41$, $Q_3=45$, $Q_4=47$, $Q_5=46$		

Figure 8 tells us the followings:

1) Spectrum level of the radiated sound due to the current-drive is higher than that due to the pressure-drive by more than 30 dB.
2) Emphasis in level of second and third harmonics is outstanding in the current-drive [cf. Figs. 7 (a) and 8 (a)].

NII-Electronic Library Service

The Acoustical Society of Japan

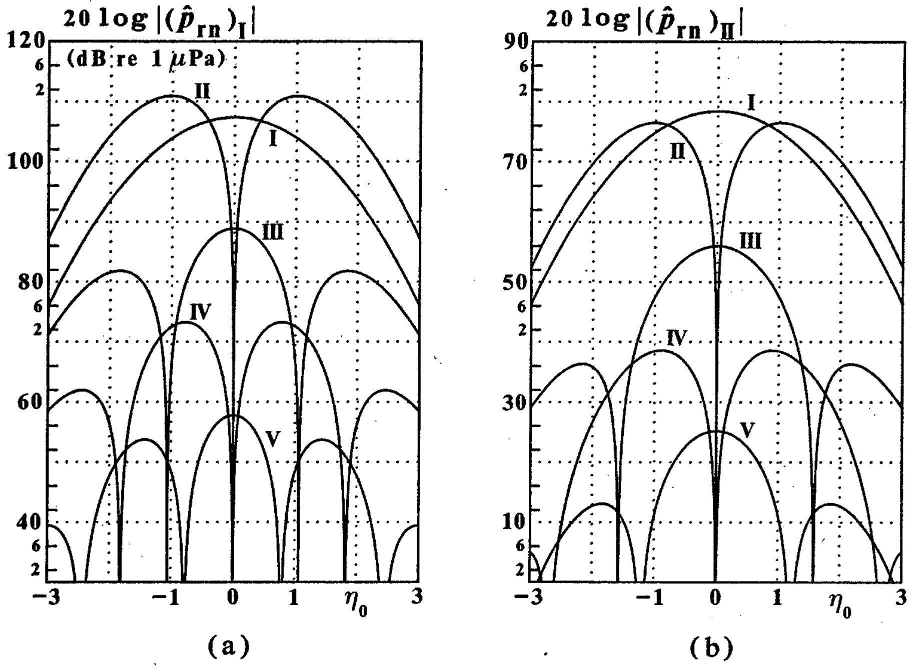

Fig. 8 Radiated sound spectrum level as a function of the normalized jet offset (unsaturated regime).
(a) Current-drive, (b) pressure-drive. The Roman numerals represent the harmonics.

3) Such an emphasis is not outstanding in the pressure-drive [cf. Figs. 7 (b) and 8 (b)].
4) Current- and pressure-drives have different offset values at which minimum levels of each harmonic occur.
5) Deep troughs in harmonic generation due to the current-drive are therefore somewhat compensated by the harmonic generation due to the pressure-drive.

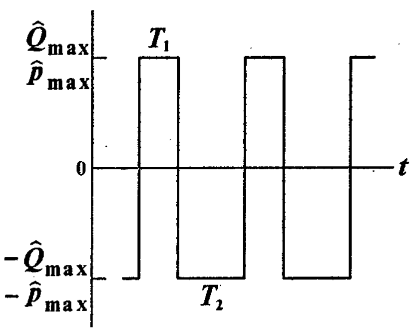

Fig. 9 Completely switching jet.
During time interval T_1 within an oscillation period, the jet flows into the pipe and produces maximum driving flow $\hat{Q}_{max}$ and pressure $\hat{p}_{max}$. On the other hand, the jet flows out of the pipe during remaining time interval T_2 and produces $-\hat{Q}_{max}$ and $-\hat{p}_{max}$.

6. SATURATED REGIME

6.1 The Jet

It may be considered that the jet flow into the pipe continues to increase as far as jet oscillation amplitude grows and jet velocity increases. However, this jet driving flow will saturate at given amplitude and velocity. Saturation of jet driving flow then causes saturation of acoustic output, that is, the maximum level of radiated sound.

Jet oscillation amplitude is usually much larger than the jet offset at the saturated state. The jet thus spends a period of its oscillation almost completely outside and inside the pipe. A time crossing the edge can be ignored. Such a completely switching action of the jet is shown in Fig. 9. The jet alternately flows into and out of the pipe during time intervals T_1 and T_2 respectively. From Eq. (2) maximum driving flow $\hat{Q}_{max}$ may be approximated by

$$\hat{Q}_{max} \simeq (b\sigma U_e)\int_0^\infty g(\eta)d\eta\,. \tag{37}$$

If we suppose Gaussian distribution of Eq. (32),

$$\hat{Q}_{max} \simeq \sqrt{\pi/2}\,(b\sigma U_e)\,. \tag{38}$$

Similarly, from Eq. (8) we get the following maximum

NII-Electronic Library Service

driving pressure $\hat{p}_{max}$ at the same time:

$$\hat{p}_{max} \simeq (b\sigma/S_p)(\rho U_e^2)\int_0^\infty g^2(\eta)d\eta = (\sqrt{\pi}/2)(b\sigma/S_p)(\rho U_e^2)\,. \tag{39}$$

By the way, a jet is produced by receiving momentum from an external source and then being ejected from an orifice or slit. Resultant jet spreads out into the surrounding fluid as it goes downstream. During this spreading process the jet exerts no force on any external fluid, and vice versa. Total momentum flux of the jet is thus conserved at any downstream position x. This must be the case whether the jet is laminar or turbulent.

Since our jet is two-dimensional, we consider the momentum flux M per unit width. Then,

$$M(x) = \rho\int_{-\infty}^\infty U^2(x, y)dy = \text{const.} \tag{40}$$

From Eqs. (1) and (40) we get the following relation between the momentum fluxs at the flue slit and at the edge:

$$\rho U_0^2 h = \rho U_e^2 \sigma\int_{-\infty}^\infty g^2(\eta)d\eta\,,$$

therefore we can express the effective jet thickness σ at the edge as

$$\sigma = h(U_0/U_e)^2\left[\int_{-\infty}^\infty g^2(\eta)d\eta\right]^{-1}, \tag{41}$$

where U_0 and h are jet velocity and jet thickness at the flue respectively. Gaussian jet distribution gives

$$\sigma = (h/\sqrt{\pi})(U_0/U_e)^2\,. \tag{42}$$

From Eqs. (38) and (42) we can rewrite $\hat{Q}_{max}$ as

$$\hat{Q}_{max} \simeq [\sqrt{2}\,(U_0/U_e)][(1/2)bhU_0]\,. \tag{43}$$

This equation tells us that jet driving flow $\hat{Q}_{max}$ into the pipe equals $\sqrt{2}\,(U_0/U_e)$ times half an initial flow $(1/2)bhU_0$ at the flue if the Gaussian velocity distribution is assumed. And we know maximum driving flow increases in proportion to the square of initial jet velocity U_0. Since factor $\sqrt{2}\,(U_0/U_e)$ is greater than 1, Eq. (43) indicates that the amount of jet flow increases as the jet travels downstream. The jet draws ambient fluid into itself from the sides. This is generally known as entrainment effect.

On the other hand, the jet driving pressure is reduced by the ratio of cross sectional areas:

$$\hat{p}_{max} \simeq (bh/S_p)[(1/2)\rho U_0^2]\,, \tag{44}$$

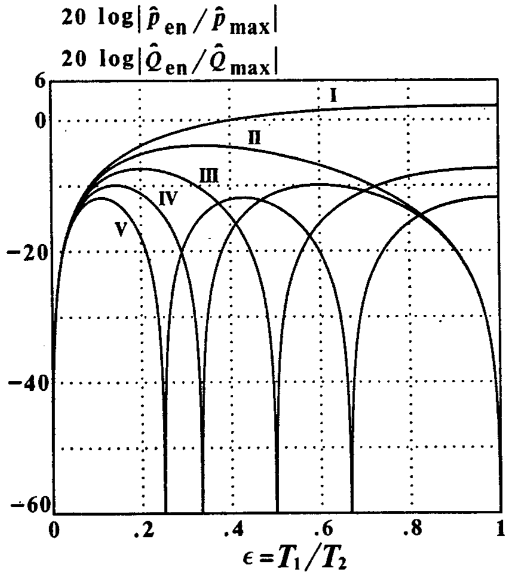

Fig. 10 Jet source spectrum level as a function of time interval ratio ϵ of jet switching action (saturated regime). The Roman numerals represent the harmonics.

where Eqs. (39) and (42) are employed. This equation is just conservation law of total jet momentum flux.

6.2 Calculation of Jet Source Spectrum

Time intervals T_1 and T_2 of jet switching action may be determined by the flow resistances which the jets into and out of the pipe suffer respectively.[12,17] Although the effect of offset becomes weak in the saturated regime, it can not be ignored at all if the offset is relatively large. In our calculation we set $T_1 = \epsilon T_2$ for the simplicity. The value of interval ratio ϵ may be smaller than 1 generally, because the resistance to the flow into the pipe may be considerably greater than that to the flow into the free space. Fourier series expansion of the function shown in Fig. 9 gives the following source spectrums $\hat{Q}_{en}$ and $\hat{p}_{en}$ respectively:

$$\hat{Q}_{en} = (4/n\pi)\hat{Q}_{max}\sin[n\pi(\epsilon/(1+\epsilon))]\,, \tag{45}$$

$$\hat{p}_{en} = (4/n\pi)\hat{p}_{max}\sin[n\pi(\epsilon/(1+\epsilon))]\,. \tag{46}$$

In Fig. 10 we draw the relative source spectrum levels of $|\hat{Q}_{en}/\hat{Q}_{max}|$ and $|\hat{p}_{en}/\hat{p}_{max}|$, which have the same functional form, as functions of interval ratio ϵ. Instead of jet offset in the unsaturated regime, time interval ratio of jet switching action becomes a decisive factor determining organ pipe harmonic structure in the saturated regime.

NII-Electronic Library Service

The Acoustical Society of Japan

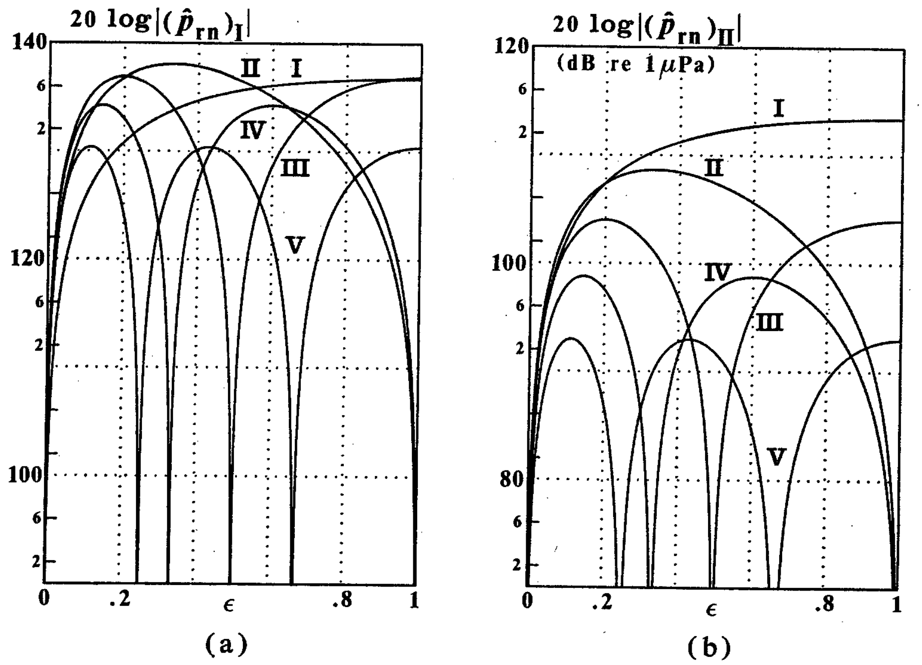

Fig. 11 Radiated sound spectrum level as a function of the jet switching time interval ratio (saturated regime).
(a) Current-drive, (b) pressure-drive. The Roman numerals represent the harmonics.

6.3 Radiated Spectrum

Jet source spectrums of Eqs. (45) and (46) are transformed into the following radiated spectrums according to Eqs. (12), (13), and (24):

$$(\hat{p}_{rn})_{I}=(\hat{Q}_{en})[j(2\pi f_{s}\Delta l/c)nY_{n}][(\rho f_{s})n]\,, \qquad (47)$$

$$(\hat{p}_{rn})_{II}=(\hat{p}_{en})[(S_{p}/\rho c)Y_{n}][(\rho f_{s})n]\,. \qquad (48)$$

We plot their logarithmic levels (relative to 1 μPa) in Fig. 11 as functions of switching interval ratio ϵ. Jet velocity measurement on model CP-I gave $U_0=21$ m/s and $U_e=6$ m/s near the saturated regime.[1] Other parameter values to draw Fig. 11 are the same as in Table 1. Note that jet offset and jet deflection amplitude are not essential (and thus ignored) in the saturated regime as a limiting state.

Figure 11 tells us the followings:

1) Spectrum level of the radiated sound due to the current-drive is higher than that due to the pressure-drive by more than 25 dB [cf. Figs. 11 (a) and (b)].
2) Development of higher harmonics is fully attained in the saturated regime of current-drive [cf. Figs. 8 (a) and 11 (a)].
3) Such development is not full in the pressure-drive.
4) A few values of ϵ, which are the same in the current- and pressure-drives, bring null level of higher harmonics.

The value of ϵ may be principally determined by the pipe geometry and secondarily by the geometries of the flue slit and mouth. Flow resistance into the pipe depends on the ratio of pipe length to pipe cross section.[12,17] Wider pipes with a given length will give larger interval ratios. Therefore from Fig. 11 we may state the followings:

5) Extremely wide pipe ($\epsilon\simeq1$) radiates only odd harmonics.
6) Relatively wide pipe ($\epsilon\simeq0.8$) radiates low levels of even harmonics. Levels from the first to the fifth harmonic are in order 136, 128, 135, 130, and 126 dB *re* 1 μPa.
7) Considerably narrow pipe ($\epsilon\simeq0.2$) radiates high levels of higher harmonics. Levels from the first to the fifth are in order 131, 137, 137, 133, and 124 dB.

Limiting tone colour peculiar to a given organ pipe in the fully saturated regime is principally attributed to its pipe geometry which determines the jet switching interval ratio, pipe resonance or filtration characteristics, and radiation characteristics.

7. CONCLUSION

A general approach to the total picture of the

NII-Electronic Library Service

The Acoustical Society of Japan

harmonic generation mechanism in organ pipes has been developed. The mechanism consists of three elementary processes: source spectrum generation by the jet, filtration by the normal mode resonance of the mouth-pipe system, and radiation from the openings of the mouth and pipe end. In the consideration of harmonic generation, our theoretical treatment contains the excitation mechanisms due to the current- and pressure-drives, and classifies them into the unsaturated and saturated regimes.

In the unsaturated regime, the desicive causes originating the source spectrum are the asymmetrical jet-edge configuration and lateral jet velocity distribution. The asymmetry is represented as the offset of the jet center plane relative to the edge. Contribution of the pressure-drive to the harmonic generation is insignificant in most cases. The essential features of the harmonic structure and its development are clearly formulated in the matrix form.

In the fully saturated regime, the decisive factor determining the harmonic structure is the ratio of time intervals in which the jet deflects completely inside and completely outside the pipe. The jet offset and velocity distribution now become almost unessential. The effective thickness of the switching jet which governs the harmonic level is deduced from the conservation law on the total momentum flux of the jet. Because the interval ratio depends on the geometries of the pipe, mouth, and flue slit, they participate in producing a limiting tone colour peculiar to an organ pipe itself.

Our theory makes possible to predict the harmonic structure and sound level of the radiated tone. Moreover, it may present the acoustical foundation for the voicing adjustment and the construction of various organ pipe ranks. Although this paper is restricted to a theoretical study, fundamental aspects revealed in it will be followed by the experimental study.

REFERENCES

1) S. Yoshikawa and J. Saneyoshi, "Feedback excitation mechanism in organ pipes," J. Acoust. Soc. Jpn. (E) **1**, 175–191 (1980).
2) S. Yoshikawa and J. Saneyoshi, "Analysis of excitation mechanisms in musical instruments," J. Acoust. Soc. Jpn. **37**, 543–550 (1981) (in Japanese).
3) L. Cremer and H. Ising, "Die selbsterregten Schwingungen von Orgelpfeifen," Acustica **19**, 143–153 (1967/68).
4) J. W. Coltman, "Sounding mechanism of the flute and organ pipes," J. Acoust. Soc. Am. **44**, 983–992 (1968).
5) A. H. Benade and D. J. Gans, "Sound production in wind instruments," Ann. N. Y. Acad. Sci. **155**, 247–263 (1968).
6) N. H. Fletcher, "Nonlinear interactions in organ flue pipes," J. Acoust. Soc. Am. **56**, 645–652 (1974).
7) Lord Rayleigh (J. W. S. Strutt), *The Theory of Sound* (Dover, New York, 1945), Vol. 2, pp. 384.
8) Y. Andō, "Drive conditions of the flute and their influences upon harmonic structure of generated tone (An experimental study of the flute II)," J. Acoust. Soc. Jpn. **26**, 297–305 (1970) (in Japanese).
9) A. W. Nolle, "Some voicing adjustments of flue organ pipes," J. Acoust. Soc. Am. **66**, 1612–1626 (1979).
10) N. H. Fletcher and L. M. Douglas, "Harmonic generation in organ pipes, recorders, and flutes," J. Acoust. Soc. Am. **68**, 767–771 (1980).
11) S. Yoshikawa, "Harmonic generation mechanism in organ pipes I," The Autumn Meeting of the Acoustical Society of Japan, 673–674 (1980) (in Japanese).
12) von E. G. Schlosser, "Tonerzeugung und Toncharakteristika bei Labialpfeifen," Acustica **43**, 177–187 (1979).
13) N. H. Fletcher, "Jet-drive mechanism in organ pipes," J. Acoust. Soc. Am. **60**, 481–483 (1976).
14) A. H. Benade, "On woodwind instruments bores," J. Acoust. Soc. Am. **31**, 137–146 (1959).
15) N. H. Fletcher, "Scaling rules for organ flue pipe ranks," Acustica **37**, 131–138 (1977).
16) Lord Rayleigh (J. W. S. Strutt), *The Theory of Sound* (Dover, New York, 1945), Vol. 2, pp. 66–68.
17) H. Dänzer and W. Kollman, "Über die Strömungsverhältnisse an der Lippenöffnung von Orgelpfeifen," Z. Phys. **144**, 237–243 (1956).

NII-Electronic Library Service